Measurement Science
and Technology

PURPOSE-LED
PUBLISHING™

PAPER • OPEN ACCESS

Laser absorption spectroscopy for traceable dynamic pressure measurement in shock tubes: an inter-laboratory comparison

To cite this article: Eynas Amer *et al* 2026 *Meas. Sci. Technol.* **37** 405010

View the article online for updates and enhancements.

You may also like

- Comparison of line width calibration using critical dimension atomic force microscopes between PTB and NIST
Gaoliang Dai, Kai Hahm, Harald Bosse et al.
- Optical power scale realization using the predictable quantum efficient detector
Kinza Maham, Petri Kärhä, Farshid Manoocheri et al.
- Toxic air pollution and concentrated social deprivation are associated with low birthweight and preterm Birth in Louisiana
Kimberly A Terrell, Gianna N St Julien and Maeve E Wallace

This content was downloaded from IP address 192.71.100.250 on 16/10/2026 at 13:29

Measurement Science and Technology

Check for updates

PAPER

OPEN ACCESS

RECEIVED
23 June 2026

REVISED
3 September 2026

ACCEPTED FOR PUBLICATION
22 September 2026

PUBLISHED
7 October 2026

Original content from this work may be used under the terms of the Creative Commons Attribution 4.0 licence.

Any further distribution of this work must maintain attribution to the author(s) and the title of the work, journal citation and DOI.

Laser absorption spectroscopy for traceable dynamic pressure measurement in shock tubes: an inter-laboratory comparison

Eynas Amer[1,*], **Denghao Zhu**[2,3,*], **Sumit Agarwal**[2], **Fredrik Arrhén**[1] and **Zhechao Qu**[2,*]

[1] Measurement Science and Technology, RISE Research Institutes of Sweden, Borås, Sweden
[2] Physikalisch-Technische Bundesanstalt (PTB), Braunschweig, Germany
[3] Current address: School of Energy and Environment, Southeast University, Nanjing, People's Republic of China.
[*] Authors to whom any correspondence should be addressed.

E-mail: eynas.amer@ri.se, denghao.zhu@seu.edu.cn and zhechao.qu@ptb.de

Keywords: dynamic pressure, shock tube, laser absorption spectroscopy, dynamic calibration, inter-laboratory comparison

Abstract

In this study, the shock tubes at RISE and PTB were validated at low pressure region (up to 200 kPa) and frequency up to 100 kHz by an inter-laboratory comparison using two transfer standards (TSs). Shock tubes can generate step-like pressure pulses at the end-wall plate of the driven section where the device under test is mounted. The generated reference step pressure is assumed to have the shape of a Heaviside step function. Therefore, the pressure amplitude can be calculated using the Rankine–Hugoniot step relations with the knowledge of the Mach number of the incoming shock wave and the initial static pressure of the gas medium. In this case, the shock tube is considered as a primary standard. On the other hand, shock tube can be used as a generator of repeatable reference pressure steps while its amplitude is measured using other primary methods, such as laser absorption spectroscopy. In this work, the respective shock tubes at RISE and PTB were used as both primary standards and pressure generators where laser absorption spectroscopy method was deployed to measure the reference pressure amplitudes. Two TSs were characterized at RISE and PTB facilities, and their dynamic responses were calculated at different pressure amplitudes and the associated uncertainty budgets were evaluated. The comparison between the shock tube results obtained at RISE and PTB showed good consistency.

1. Introduction

Despite the importance of dynamic pressure measurements, traceable dynamic calibration of pressure measurement systems (PMSs) is presently lacking. Dynamic PMSs are currently calibrated quasi-statically, reporting sensitivity only with respect to pressure. Quasi-static methods assume that the PMS responds in the same way for dynamic pressure as for static pressure, which may result in significant errors for the users. For accurate and reliable measurements, the PMS that are used in applications where pressure varies with time should be calibrated dynamically. To establish traceability for dynamic pressure calibration, developing new and validating the existing standards and methods are vital. Several National Metrology Institutes (NMIs) and calibration laboratories are working to establish a traceability chain [1–7]. Shock tubes are the available candidates to realize high-frequency reference pressures up to megahertz. Shock tubes have limitations at the lower ends for both amplitude and frequency, respectively. In shock tubes, the amplitude of the reference pressure is calculated using a theoretical model, an experimental validation of this model is missing. Quantum-based methods are very useful tools to assess pressure [8], since they are based on the unique properties of the pressure medium molecules.

Under dynamic pressure conditions, both pressure and temperature change very rapidly with time, making the use of quantum-based methods to assess pressure challenging. In this work, tunable diode laser absorption spectroscopy (TDLAS) was used to measure dynamic pressure and temperature simultaneously. TDLAS has been a well-established technique used as a tool to measure gas concentration and temperature in many applications [9, 10]. When a radiation (i.e. laser beam) of the same photon energy

© 2026 The Author(s). Published by IOP Publishing Ltd

as one of the vibration/rotation transitions of the medium gas molecule interacts with the molecule, the molecule vibrates/rotates and then returns to the equilibrium state by re-radiates that energy but in a random direction. By measuring the absorption line-shape at specific vibrational/rotational transition, the medium gas pressure can be determined. The medium temperature can be measured simultaneously from the ratio of two lines intensities with different lower-state energy. If the medium molecules achieve thermal equilibrium faster than the time scale of pressure changing, the absorption line-shapes under transient conditions are the same as they would be in steady conditions.

Recent studies have demonstrated the feasibility of spectroscopic pressure diagnostics in a variety of harsh and transient environments. Nair *et al* developed a high-speed optical pressure-sensing technique based on mid-infrared laser absorption spectroscopy of CO near 5 μm. Their method exploited the linear relationship between pressure and collisional broadening of CO absorption lines, while a bias-tee-modulated quantum cascade laser operating at MHz scan rates enabled multiple transitions to be resolved within a single sweep. Combined with two-line thermometry, this approach allowed simultaneous pressure and temperature measurements in shock tube and detonation tube environments over 1500–3000 K and 0.05–1 MPa, with uncertainties of approximately 10% at 1 MHz [11]. Vandervort *et al* proposed a single-line absorption diagnostic based on the potassium D2 transition near 766.7 nm for rapid temperature and pressure measurements in high-enthalpy flows. By fitting the Voigt profile of a single transition, they extracted temperature from the Doppler contribution and pressure from the collisional contribution, achieving uncertainties as low as 6% in shock tube experiments [12]. More recently, Gessman *et al* developed a water-vapor-based optical pressure diagnostic for post-detonation environments using a MEMS-VCSEL scanning over 7350–7900 cm^{-1} at 100 kHz. By fitting broadened H_2O spectra under 0.025–6.8 MPa and 293–2300 K conditions, they reported average errors of 2.6% for temperature and 5.4% for pressure, while also quantifying the influence of simplified broadening models in compositionally uncertain environments [13].

Taken together, these studies clearly demonstrate that absorption-spectroscopy-based methods can provide rapid, non-intrusive pressure diagnostics under extreme transient conditions. However, most of the existing work has been developed primarily from the perspective of engineering diagnostics, with emphasis on measurement feasibility, sensitivity, and application-specific performance. Comparatively less attention has been paid to the metrological foundation of such measurements, especially with respect to traceability, calibration hierarchy, transfer standards (TSs), and comprehensive uncertainty evaluation. In other words, while spectroscopic approaches have shown considerable promise as dynamic pressure sensors, they have not yet been fully established as traceable dynamic pressure measurement methods.

A significant step toward this goal was made by Douglass and Olson, who proposed a fundamentally different concept: using laser absorption spectroscopy not merely as an engineering sensor, but as a primary standard approach for dynamic pressure metrology [14]. Their vision was to establish traceable calibration for transient pressure measurements, an area in which no NMI had yet provided a complete solution. The method relied on the quantum-mechanical properties of molecular absorption lines, with pressure inferred from Lorentzian collisional broadening and temperature from line-intensity ratios. Using wavelength modulation spectroscopy of CO_2 near 1610 nm as a proof of concept, they demonstrated optical pressure measurements that agreed with capacitance-based sensors to within 0.6% on average under steady conditions and showed linewidth repeatability of 0.5% with 10 averages at 400 Hz. More importantly, they outlined a pathway toward extending the method to CO in helium at 100 kHz with an expanded uncertainty of 5%, thereby linking steady-state primary pressure standards to transient measurements through molecular lineshape parameters as transfer quantities.

Despite this important conceptual advance, systematic traceability to dynamic pressure standards remains generally lacking. From a metrological standpoint, dynamic pressure measurement is still hindered by the absence of well-established calibration techniques and traceable reference standards for transient signals. As a result, comprehensive uncertainty analyses for TDLAS-based dynamic pressure measurements remain limited, and further work is needed to rigorously assess their accuracy, equivalence, and traceability across facilities. The novelty of this work lies in using laser absorption spectroscopy as an independent, traceable dynamic pressure reference for shock-tube-based calibration of pressure TSs. In this paper, the shock tubes at RISE and PTB were validated by performing a comparison using two TSs. Two methods were used to calculate the reference pressure at each facility; namely shock tube model and laser absorption spectroscopy. The sensitivity of the respective TSs was calculated at each facility, and the corresponding uncertainty budget was assessed. A comparison of the results was done, and the degree of equivalence was calculated.

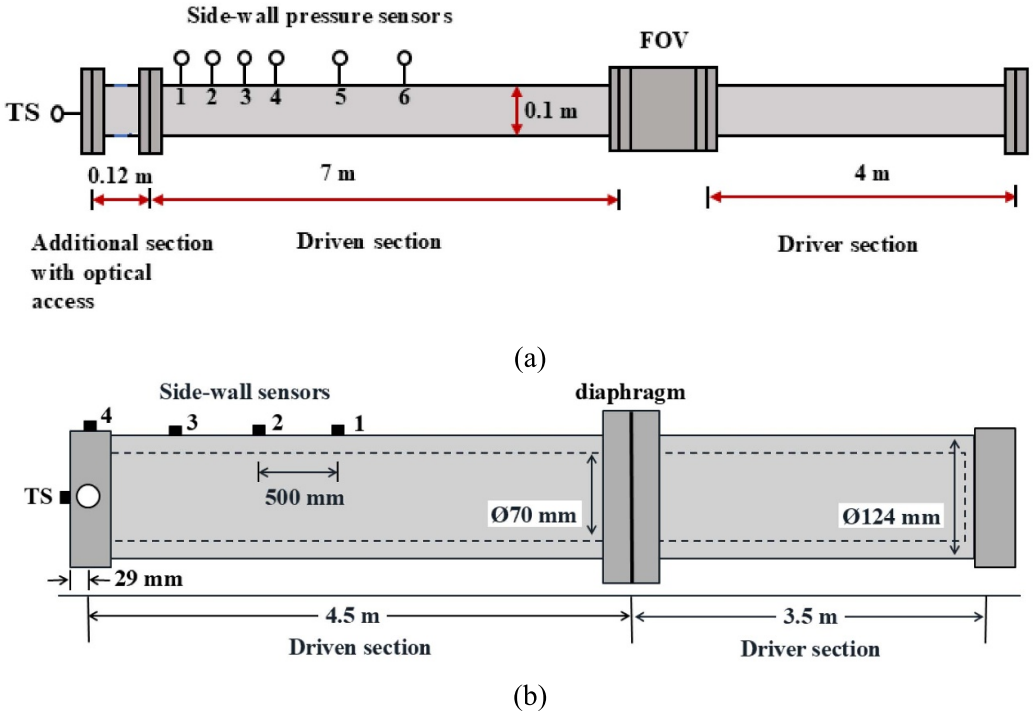

Figure 1. An illustration of the shock tube at (a) RISE, (b) PTB, TS: transfer standard, FOV: fast-opening valve.

2. Experimental setup

Shock tubes coupled with the laser absorption spectroscopy setup for dynamic pressure measurements at RISE and PTB, respectively, are described in the following sections. An illustration of the shock tube at RISE and PTB is shown in figures 1(a) and (b), respectively.

2.1. RISE facility

A laser absorption spectroscopy method for measuring dynamic pressure was developed at RISE. A distributed feed-back (DFB) laser (Nanoplus GmbH) was used to excite a CO_2 transition of $\nu_1 + \nu_3$ vibration band $R(28)$ centered at 3633.08 cm^{-1}. The wavelength of the laser can be tuned by varying the injection current and/or temperature using the laser controller (LDC501, SRS). The laser current was modulated by a linear ramp at a scan rate up to 3 kHz supplied by a function generator (AFG1062, Tektronix). A solid germanium etalon of 50.8 mm length was used to measure the wavelength tuning of the laser. The etalon transmission peaks were adapted to convert the signal from the time domain to the wavenumber domain. However, the absolute wavenumber was calibrated by the well-known position of the CO_2 transition from the HITRAN database [15]. The laser beam was focused onto a photodetector (PDAVJ8, Thorlabs) after passing through the gas medium.

To optimize the settings of the laser controller and calculate the spectroscopic parameters, static measurements were performed using a heated 10 cm long single-pass static gas cell. A gas mixture of 1% CO_2 and 99% Ar was used as a pressure medium. Before the measurements, the gas cell was evacuated using a vacuum pump (NeoDry 15E, Kashiyama) and flushed by the gas mixture three times to ensure the well-known gas composition inside the gas cell. A calibrated pressure transducer (VPM-15, Sens4) was employed to measure the static pressure. To control the gas temperature, the gas cell was equipped with a digital temperature control module which was calibrated using a calibrated PT100. A photo of the static setup is shown in figure 2.

For dynamic pressure measurements, the laser absorption spectroscopy setup was coupled to the shock tube. The shock tube at RISE consists of a 4 m driver section and a 7 m driven section, separated by a fast-opening valve, with an inner diameter of 10 cm. A full description of the shock tube can be found in [16]. For the spectroscopic measurements, an additional section with the same inner diameter as the shock tube (10 cm) and a length of 12 cm was connected to the shock tube, see figure 1(a). The additional section has an optical access of two CaF_2 windows (diameter = 38.1 mm, thickness = 6 mm)

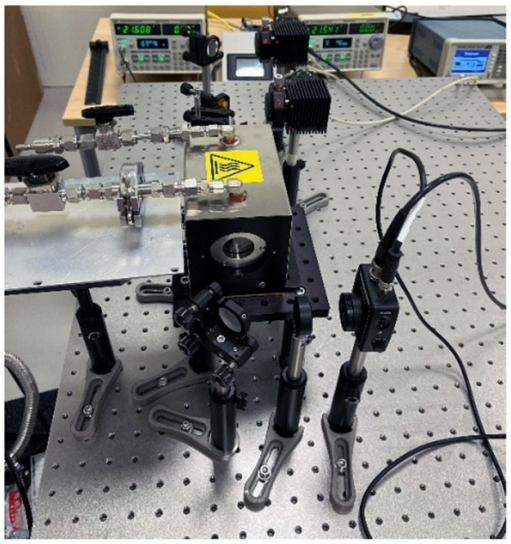

Figure 2. A photo of the laser absorption spectroscopy setup coupled to the static gas cell at RISE.

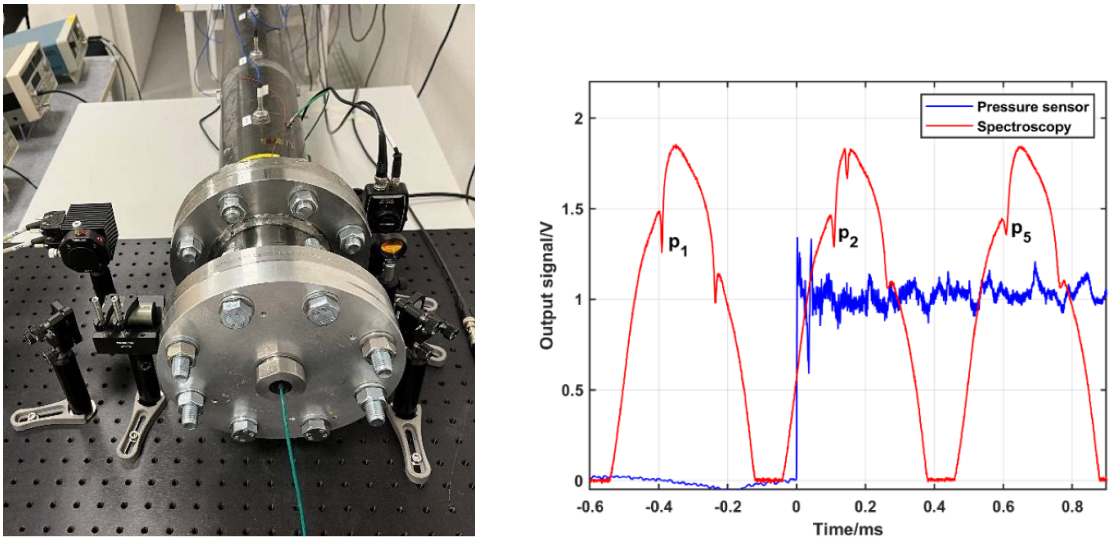

Figure 3. (a) A photo of the laser absorption spectroscopy setup coupled to the shock tube at RISE; (b) Typical recorded signals using a mixture of 1% CO_2 + 99% Ar as a driven gas at a nominal step pressure of 100 kPa, the scanning rate was 2 kHz.

opposite each other centered at 5 cm from the end wall plate of the driven section where the respective TSs were flush mounted. The laser beam was focused onto the photodetector after passing through the shock tube perpendicular to the shock wave propagation direction. A photo of the setup is depicted in figure 3(a).

The output signals from the respective TSs, the photodetector, and the side-wall sensors were simultaneously acquired using an 8 channel 12 bit 60 MS s^{-1} per channel oscilloscope (PXI-5105, NI) with a maximum sampling size of 10^6 samples. The LabVIEW 2019 software was used for data acquisition. A typical recorded CO_2 absorption spectrum at 3633.08 cm^{-1} at a nominal step pressure of 100 kPa with a mixture of 1% CO_2 + 99% Ar as a driven gas with pressure p_1 of 30 kPa is shown in figure 3(b).

2.2. PTB facility

The shock tube at PTB comprises a 3.5-meter driver section and a 4.5 m driven section, separated by aluminum diaphragms, with an inner diameter of 70 mm. The initial pressure (p_1) of the gas mixture charged into the driven section was measured by a pressure sensor (MKS Baratron, 0–1000 mbar). The shock-heated pressure was measured using five sensors (603CAB, Kistler) and charge amplifiers (5018 A,

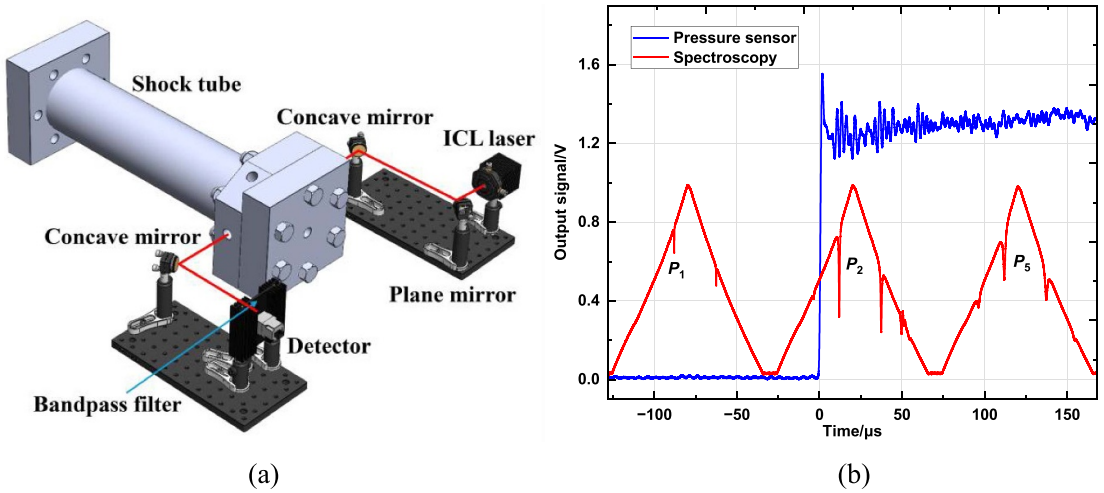

Figure 4. (a) Schematic of the shock tube experimental setup at PTB; (b) Measurement using the shock tube with 1% CO + 1% H_2 + 98% Ar at $p_1 = 2.5$ kPa.

Kistler). Gas mixtures were prepared in a 50 l stainless steel tank, vacuumed to 1×10^{-7} mbar before mixing. Target gases flush the system twice to remove residuals, and mixtures are homogenized using a magnetic stirrer (Cyclone 300ac, Büchiglasuster) for at least two hours.

Figure 4(a) shows the coupling of shock tube and TDLAS setup in three-dimensional view. For laser diagnostics, two ZnSe windows are installed opposite each other at the fourth pressure sensor's plane. A continuous-wave distributed-feedback interband cascade laser (CW-DFB-ICL, Nanoplus) was used to cover two CO transitions in the fundamental $v = 1 \leftarrow 0$ band of $P(20)$ centered at 2059.91 cm^{-1} and $P(14)$ centered at 2060.33 cm^{-1}. They are selected for temperature measurement using two-line thermometry while only CO transition of $P(20)$ was used for pressure quantification. The laser wavelength was tuned by a laser diode controller (PRO8000 equipped with LDC8002 and TED8020, Thorlabs) together with a function generator (KEYSIGHT, 33500B). The tuning frequency was set as 10 kHz with a triangle-shaped current ramp. A detector (PVI-4TE-5, VIGO) was used to receive the laser signal focused by a concave mirror (CM508-050-M01, focal length: 50 mm, Thorlabs). To ensure accurate wavelength calibration, a reference beam was directed through a Germanium etalon (76.244 mm length, calibrated by PTB) to monitor the laser tuning. The etalon transmission peaks enabled precise conversion of the time-domain signal into wavenumber space. A narrow bandpass filter (CWL = 4856 nm, BW = 30 nm, Laser Components) was placed in front of the detector to separate the signal from the thermal emission from the shock-heated gases. The pressure and photodetector signals were recorded by a 16-bit 80 MS s^{-1} data acquisition card (M2p.5943-x4, Spectrum Instrumentation).

Measurements performed using the shock tube with a mixture of 1% CO + 1% H_2 + 98% Ar as a driven gas with pressure p_1 of 2.5 kPa is depicted in figure 4(b). Here a small portion of H_2 (1%) was added to reduce the vibrational relaxation time of CO behind the reflected shock wave.

2.3. The TSs and the experimental settings

Two TSs were characterized at RISE and PTB shock tube facilities, respectively:

- TS1: Kistler 4017 A piezoresistive sensor and signal conditioner Kistler 4624 A, maximum pressure 0.5 MPa (absolute) and natural frequency > 7 kHz.
- TS2: Kistler 603CAB piezoelectric sensor and charge amplifier Kistler 5018A1000, pressure range: 0 MPa—1 MPa and natural frequency > 500 kHz.

The experimental and data acquisition settings for characterizing the two TSs at RISE and PTB, respectively, are listed in table 1.

Table 1. A list of the experimental and data acquisition settings for characterizing the two TSs at the two facilities.

Facility	Driven gas	Driver gas	Sampling rate (MS/s)	Sampling size (samples)
RISE	Ar $1\%CO_2 + 99\%Ar$	Ar	3	6×10^4
PTB	$1\%CO + 1\%H_2 + 98\%Ar$ $1\%CO + 20\%He + 79\%Ar$	Ar	80	64×10^4

3. Methodology

In this work, the respective shock tubes at RISE and PTB were used to generate repeatable step-like pressure pulses at the end-wall plate of the driven section where the respective TS1 and TS2 were flush mounted. Two methods were used at RISE and PTB, respectively, to calculate the amplitude of the generated reference pressure pulses. The first method was by applying the well-established shock tube model, since the generated reference step pressure was assumed to have the shape of a Heaviside step function. Therefore, the pressure amplitude was calculated using the Rankine–Hugoniot step relations with the knowledge of the Mach number of the incident shock wave and the initial static pressure of the gas medium in the driven section. In the second method, laser absorption spectroscopy was deployed to quantify the pressure by measuring the line-shape of a specific absorption of a target gas with specific concentration in a gas mixture used in the driven section.

These methods are described in the following. In addition, the uncertainty budgets in pressure calculations using the respective methods are also presented. Furthermore, the method for evaluating the equivalence between the measurements at the two facilities is depicted.

3.1. Shock tube model

Shock tube device is a potential primary standard for dynamic pressure calibration in high-frequency region. The shock tube consists of two parts; a driven section, filled with driven gas of low-pressure, p_1, and a driver section that contains a driver gas of high-pressure, p_4, separated by an opening mechanism (diaphragm or fast-opening valve). When the separation between the two parts is opened, an incident shock wave propagates in the driven section toward its end-wall plate, and an expansion wave propagates into the driver section. When the incident shock wave impinges on the end-wall plate, it reflects with pressure p_5 behind it. The pressure rises from p_1 to p_5 very rapidly (less than a microsecond) exciting all the frequencies up to hundreds of kilohertz [17]. The expansion wave reflects upon the end-wall plate of the driver section and propagates toward the driven section and interacts with the reflected shock wave. The constant-pressure time, before the interaction between the expansion and the reflected shock wave (typically from 2 ms to 5 ms) limits the lower frequency that can be realized by the shock tube. The generated reference step pressure is assumed to have the shape of a Heaviside step function. Therefore, its amplitude ($\Delta p = p_5 - p_1$) can be calculated using the Rankine–Hugoniot step relations as:

$$\Delta p = 2p_1 \frac{\gamma_1}{(\gamma_1^2 - 1)} \left(Ma^2 - 1\right) \left(\frac{Ma^2 \left(3\gamma_1 - 1\right) + 3 - \gamma_1}{Ma^2 + \frac{2}{(\gamma_1 - 1)}} \right) \tag{1}$$

where p_1 is the initial static pressure of the driven gas, γ_1 is the specific heat ratio of the driven gas and Ma is the Mach number of the incident shock wave. The Mach number is the ratio of the shock front propagation speed in the laboratory frame, u, and the speed of sound in the undisturbed driven gas $a_1 = \sqrt{\gamma_1 R_1 T_1}$, where R_1 is the specific gas constant and T_1 is the measured initial absolute temperature of the driven gas. The shock velocity at the end-wall plate can be calculated by quadratic fitting of the time of arrival (t) of the shock front at the side-wall sensors and the positions of the corresponding sensors with respect to the end-wall plate (d). A detailed description of the calculation of u can be found in [16].

3.2. Laser absorption spectroscopy

For laser absorption spectroscopy, the transmitted intensity $I_t(\nu)$ of a monochromatic laser source through a gaseous sample is given by Beer–Lambert law:

$$I_t(\nu) = E(t) + I_0(\nu) \cdot \eta(t) \cdot \exp\left[-\alpha(\nu)\right] \tag{2}$$

with the background emission $E(t)$ at time t, initial laser intensity $I_0(\nu)$, absorbance $\alpha(\nu)$, and the broadband transmission losses $\eta(t)$, which are synchronously derived from the individual raw signals and absorption profiles. The exponential term can be computed as:

$$\alpha(\nu) = -\ln\left(\frac{I_t(\nu) - E(t)}{I_0(\nu)\cdot\eta(t)}\right). \tag{3}$$

The Voigt function can be used to model the line shape of the absorbance spectrum in equation (3), which considers the combined effects of Doppler and collisional broadening on the spectral line. These effects are characterized by the Doppler broadening full width at half maximum (FWHM), $\Delta\nu_D$, and the collisional-broadening FWHM, $\Delta\nu_L$, given by:

$$\Delta\nu_D = \nu_0 \cdot \sqrt{\frac{8\cdot k_B \cdot T.\ln 2}{M\cdot c^2}} \tag{4}$$

$$\Delta\nu_L = 2\times p\times\left[\gamma_s\times x_s\times\left(\frac{T_0}{T}\right)^{n_s} + \sum\gamma_{fi}\times x_f\times\left(\frac{T_0}{T}\right)^{n_{fi}}\right] \tag{5}$$

where k_B is the Boltzmann constant with a value of $1.380\ 649\times10^{-23}$ J K^{-1}, T is the temperature, M is the molecular mass of the absorbing specie, c is the speed of light, p is the pressure, x_s and x_f are the mole fractions of the absorbing and the foreign species, γ_s and γ_{fi} are the self and foreign broadening coefficients at reference temperature T_0 (296 K), n_s and n_{fi} are the temperature dependence coefficients of self and foreign broadening coefficients.

Clearly, the absolute pressure of the reflected shock can be derived from equation (5) once the FWHM of the collisional-broadening, mole fraction, temperature and spectroscopic parameters are determined. For collisional-broadening FWHM, it can be derived from the absorption line. The mole fraction x can be pre-defined according to the gas matrix. The molecular spectroscopic parameters can be obtained from such as HITRAN database [15]. Besides, the temperature can be inferred based on two-line thermometry by calculating the integrated absorbance area ratio of two molecular transitions of the same species.

At RISE, the CO_2-Ar foreign broadening coefficient was calculated using the static setup shown in figure 2 at temperature of 296 K. The absorbance spectra (in equation (3) were recorded at a series of pressure from 0.1 atm to 1 atm. The measured absorbance at each pressure level was fitted to a Voigt line shape, and the collisional-broadening FWHM was calculated from the best fit Voigt value. Figure 5(a) depicts the dependence of the collisional-broadening FWHM on the static pressure at temperature of 296 K. The CO_2-Ar foreign broadening coefficient (γ_f) was inferred from the slope of the linear fit. The measurements were repeated six times, and an average value of γ_f was determined. For dynamic pressure calculation, equation (5) was applied using the spectroscopic parameters in table 2 and T calculated from the shock tube model. The absorption of 3633.08 cm^{-1} using the shock tube at nominal p_5 of 133 kPa using a mixture of 1% CO_2 + 99% Ar as a driven gas is shown in figure 6(a).

At PTB, the foreign broadening coefficients of CO-Ar, CO-H_2 and the temperature dependence coefficients of CO-Ar were taken from the previous measurements [18]. Figure 5(b) shows the dependence of the collisional width of CO-Ar and CO-H_2 on the static pressure at temperature of 296 K. Since the temperature dependence of self-broadening is unavailable in literature, a default value of 0.5 was adopted. The rest of the spectroscopic parameters in table 2 is sourced from the HITRAN database [15]. These parameters were utilized in equation (5) to calculate the dynamic pressure where T was calculated using the two-lines thermometry method. The absorption of 2059.91 cm^{-1} using the shock tube at nominal p_5 of 140 kPa using a mixture of 1% CO + 1% H_2 + 98% Ar as a driven gas is presented in figure 6(b).

3.3. TSs dynamic response calculation

The reference step pressure calculated using the shock tube model and the laser absorption spectroscopy method, respectively, at different pressure levels was used to calculate the corresponding sensitivity of the respective TSs. Fast Fourier transform (FFT) algorithm was employed to calculate the sensitivity (the voltage output signal vs reference pressure step [20]) of the respective TSs in the frequency domain. FFT was applied to both the recorded signal from the TS and the corresponding calculated reference pressure using a Hanning window centered at pressure discontinuity of the recorded signal. The sensitivity was calculated as the magnitude of the ratio between the FFT of the signal and the FFT of the corresponding reference. The measurements were repeated three time at each pressure level, and an average value was estimated. The FWHM of Hanning window was adjusted according to the constant-pressure time of the reference pressure steps at the two facilities.

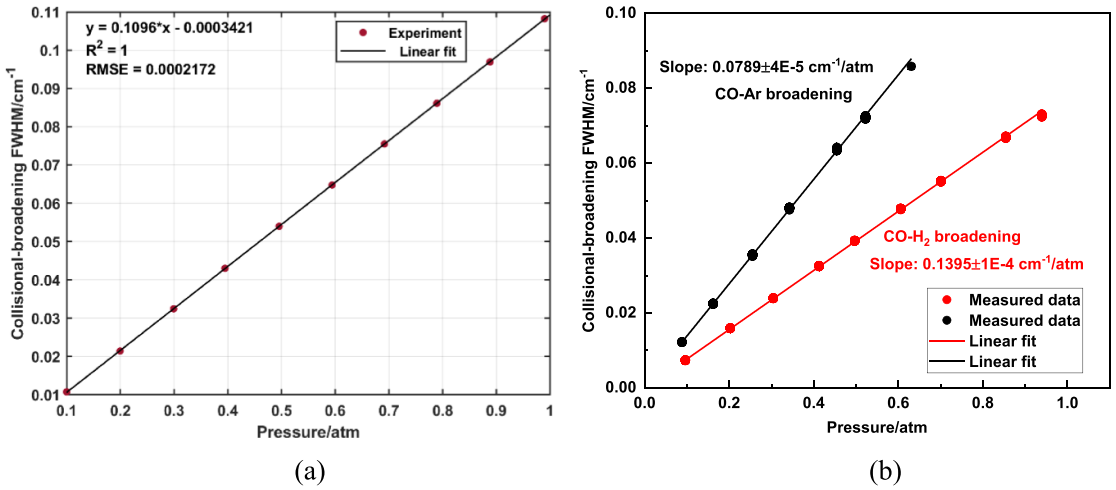

Figure 5. (a) CO_2-Ar pressure broadening coefficient for $R(28)$ using 1% CO_2 + 99% Ar (RISE); (b) CO-Ar and CO-H_2 pressure broadening coefficients for $P(20)$ using 1% CO + 1% H_2 +98% Ar (PTB) [18].

Table 2. A list of the spectroscopic parameters for the measured transitions at the corresponding facilities.

	Tracer	Transition	$2\gamma_{fi}$	$2\gamma_s$	n_f	n_s
RISE	CO_2	$R(28)$	CO_2-Ar 0.1098 (measured)	0.171 (literature [19])	0.658 (literature [19])	0.654 (literature [19])
PTB	CO	$P(20)$	CO-Ar 0.0789 [18] (measured) CO-H_2 0.1395 [18] (measured)	0.108 (literature [15])	CO-Ar 0.60484 [18] (measured) CO- H_2 0.62 (literature [18])	0.5 (default)

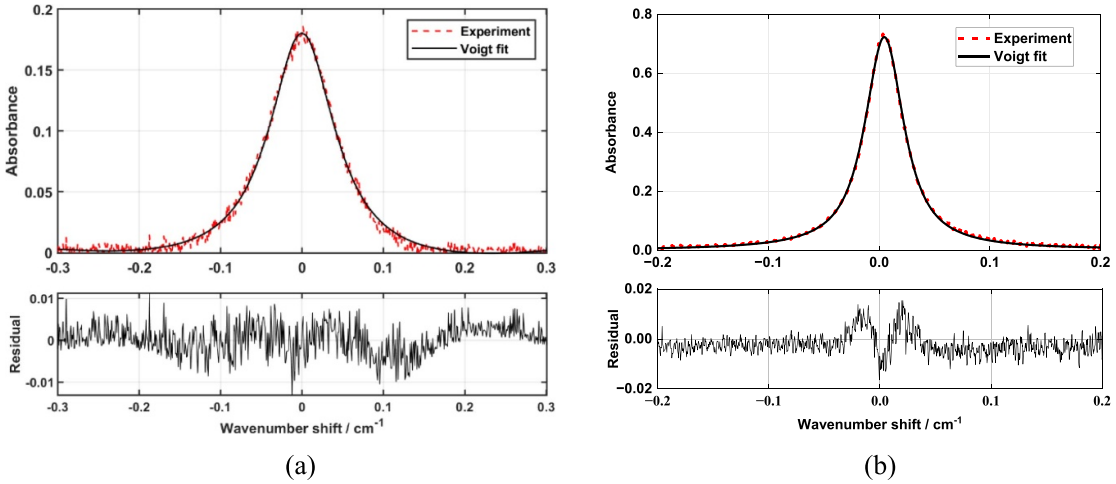

Figure 6. (a) The absorption of 3633.08 cm^{-1} at nominal p_5 of 133 kPa using a mixture of 1% CO_2 + 99% Ar as a driven gas, RISE facility; (b) The absorption of 2059.91 cm^{-1} at nominal p_5 of 140 kPa using a mixture of 1% CO + 1% H_2 + 98% Ar as a driven gas, PTB facility.

3.4. Uncertainty budget

The uncertainty budget at the two facilities for calculating the reference pressure amplitude using both the shock tube model and the laser absorption spectroscopy method, respectively, was estimated in accordance with JCGM 100:2008 [21].

Table 3. A list of the input parameters for Δp calculation and their corresponding standard uncertainty ($k = 1$), RISE.

Parameter	Standard uncertainty, $k = 1$		Distribution	Contribution %
T_1 (K)	0.45	The maximum variance between the three thermocouples readings along the driven section.	Normal	0.72
	0.05	The standard uncertainty from the calibration of the temperature measurement system.	Normal	
γ_1	10^{-3}	From literature.	Rectangular	0.10
t (s)	0.2×10^{-6}	Time resolution.	Rectangular	84.18
	0.5×10^{-6}	Maximum residual from the curve fitting.	Normal	
d (m)	10^{-4}	The standard uncertainty from the sensors positions measurements.	Normal	10.68
p_1 (Pa)	60	The standard uncertainty from the transmitter calibration.	Normal	4.32
	6	Transmitter resolution.	Rectangular	
	63	Temperature effect.	Rectangular	
	116	Transmitter drift.	Rectangular	

Table 4. A list of the input parameters for Δp calculation and their corresponding standard uncertainty, PTB.

Parameter	Standard uncertainty, $k = 1$		Distribution	Contribution %
T_1 (K)	0.5	The standard uncertainty from the temperature measuring system calibration.	Normal	0.63
γ_1	10^{-3}	From literature.	Rectangular	0.13
t (s)	2×10^{-6}	The response time of pressure sensor.	Rectangular	76.09
d (m)	10^{-3}	The standard uncertainty from sensors positions measurements.	Normal	21.07
p_1 (Pa)	10	The standard uncertainty from transmitter calibration.	Normal	2.08

3.4.1. Uncertainty in Δp calculated using shock tube model

For estimating the uncertainty in the reference step pressure calculated using equation (1), the standard uncertainty in the input parameters listed in tables 3 and 4 were used for RISE and PTB, respectively. To assess the influence of each source on the uncertainty, RISE used the Monte Carlo method while PTB used the error propagation method. In the Monte Carlo method (RISE), Δp was calculated according to equation (1) 10^6 times with the input parameters independently and randomly distributed according to table 3. The standard deviation of the resulting distribution of Δp is the standard uncertainty in Δp. In this study, the maximum standard uncertainty ($k = 1$) in Δp calculation was about 2.20% with the uncertainty in time (residual from the curve fitting which is a pressure dependent value) and the extrapolation of the shock wave velocity as the dominant uncertainty sources.

Following the methodology described in the previous study [22], the standard uncertainty of the input parameters for Δp calculation at PTB shock tube are shown in table 4. The overall uncertainty ($k = 1$) of Δp is 2.83 %, where the major uncertainty is contributed from the extrapolated shock velocity.

3.4.2. Uncertainty in Δp calculated using laser absorption spectroscopy

The standard uncertainty in Δp calculated using the laser absorption spectroscopy method is the root of the squares' sum of the uncertainty in p_5 and p_1, respectively. The standard uncertainty in p_5 was calculated using the Monte Carlo method at both RISE and PTB. The input parameters for calculating p_5 and their respective standard uncertainties are listed in tables 5 and 6 for RISE and PTB, respectively. p_5 was calculated according to equation (5) 10^6 times with the input parameters independently and randomly distributed according to tables 5 and 6 for the calculations at RISE and PTB, respectively. The standard deviation of the resulting distribution of p_5 is the standard uncertainty in p_5.

- In table 5 the uncertainty in the collisional-broadening FWHM (Δv_L) comprises: the uncertainty in absorbance calculation, wavenumber calibration, and the Voigt profile fitting procedure.
- The foreign broadening coefficient of CO_2-Ar (γ_f) was calculated as described in section 3.2 and the uncertainty comprises the uncertainty in static pressure measurements, the uncertainty in the collisional-broadening FWHM, the residual from the curve fitting and repeatability.
- The self-broadening coefficient (γ_s), the temperature dependence coefficient of CO_2-Ar (n_f), the temperature dependence of self-broadening (n_s), were taken from the measurement results of Farooq

Table 5. A list of the input parameters for p_5 calculation using the laser absorption spectroscopy method and their corresponding standard uncertainty, RISE.

Parameter	Standard uncertainty, $k = 1$		Distribution	Contribution %
$\Delta\nu_L$	3×10^{-4}	Due to the uncertainty in absorbance calculation.	Normal	27.80
(cm^{-1})	4×10^{-4}	Due to the uncertainty in the fitting parameters of the quadratic fit for wavenumber calibration.	Normal	
	7×10^{-4}	Due to Voigt fit.	Normal	
γ_f (cm^{-1}/atm)	0.0015		Normal	63.12
γ_s (cm^{-1}/atm)	0.0025		Rectangular	0.47
n_f	0.011		Rectangular	4.57
n_s	0.009		Rectangular	0.47
x_s	6×10^{-5}		Rectangular	0.47
x_f	6×10^{-5}		Rectangular	0.47
T (K)	2		Normal	2.60

Table 6. A list of the input parameters for p_5 calculation using the laser absorption spectroscopy method and their corresponding standard uncertainty, PTB.

Parameter	Standard uncertainty, $k = 1$		Distribution	Contribution %
$\Delta\nu_L$	2.3×10^{-5}	Due to the uncertainty in absorbance calculation.	Normal	0.24
(cm^{-1})	7.1×10^{-6}	Due to the uncertainty in the fitting parameters of the quadratic fit for wavenumber calibration.	Normal	
	2.9×10^{-5}	Due to Voigt fit.	Normal	
γ_{f1} (cm^{-1}/atm)	0.000201		Normal	1.37
γ_{f2} (cm^{-1}/atm)	0.000515		Normal	<0.01
γ_s (cm^{-1}/atm)	0.00108		Rectangular	<0.01
n_{f1}	0.037		Rectangular	98.06
n_{f2}	0.031		Rectangular	0.02
n_s	0.1		Rectangular	0.21
x_s	3×10^{-6}		Rectangular	<0.01
x_{f1}	1×10^{-7}		Rectangular	<0.01
x_{f2}	1×10^{-7}		Rectangular	<0.01
T (K)	0.6	Due to the uncertainty in the calculation of absorbance.	Normal	0.09
	0.49	Due to the uncertainty in the fitting parameters of the quadratic fit for wavenumber calculations.		
	4.7	Due to Voigt fit.		

et al [19] and the stated uncertainty of the respective parameters were adapted in the uncertainty calculation.

- The uncertainty in x_s and $x_{f,}$ respectively, was based on the certified standard uncertainty from the gas supplier.
- The uncertainty in temperature was calculated using the shock tube model by applying Monte Carlo method.

From the values in table 5, the main source for uncertainty in p_5 is the foreign broadening coefficient (γ_f). By considering the uncertainty in p_1 (specified in table 3), the combined standard uncertainty ($k = 1$) in Δp calculated by the laser absorption spectroscopy method was about 2.20 %.

In table 6, the associated uncertainties of the collisional-broadening FWHM ($\Delta\nu_L$) and temperature (T) come from three main sources: the uncertainty in absorbance calculation, wavenumber calibration, and the Voigt profile fitting procedure. As mentioned above, the foreign pressure broadening coefficients of CO-Ar (γ_{f1}), CO-H_2 (γ_{f2}), and temperature dependence coefficient of CO-Ar (n_{f1}) are taken from the previous measurements [18]. The temperature dependence of self-broadening is unavailable in the literature, so that a default value of 0.5 was adopted and an uncertainty of 0.1 was assigned. The remaining spectroscopic parameters are sourced from the HITRAN database. The uncertainty in gas matrix is based on the certified standard uncertainty of the respective gas cylinder. The overall standard uncertainty ($k = 1$) of p_5 by laser absorption spectroscopy is 4.21 %, with the main contribution from n_{f1}. The uncertainty of n_{f1} measured on our previous study is 0.037, which is more than three time larger

Table 7. A list of the initial and the step parameters at each nominal reference pressure at RISE and PTB.

Facility	Nominal Δp (kPa)	P_1 (kPa)	P_4 (kPa)	p_5 (kPa)	T_5 (K)
RISE	100	30	300	130	530
PTB	100	2	23	103	2175
RISE	135	30	400	165	590
PTB	135	8	43	140	1136

comparing the uncertainty of n_f used by RISE in table 5. Currently, new experiments are being carried out at PTB to remeasure n_{f1} using a heatable high-temperature gas cell, aiming for a significantly reduced uncertainty.

The uncertainty in the sensitivity of the respective TSs was calculated according to the method described in [16].

3.5. Equivalence evaluation

The results were evaluated with respect to each TS response at each nominal pressure level in terms of sensitivity as a function of frequency. Consequently, the degree of equivalence between the two facilities was calculated according to the following [23]:

$$d_{ij} = s_i - s_j \tag{6}$$

$$U_{ij} = k\sqrt{u_c^2(s_i) + u_c^2(s_j)} \tag{7}$$

where s_i and s_j are the stated sensitivities for the two facilities i and j while $u_c(s_i)$ and $u_c(s_j)$ are the respective combined standard uncertainties in sensitivity at a nominal pressure level n. k is the coverage factor ($k = 2$). The results of the two facilities are considered as equivalent if $|d_{ij}|$ is less than the expanded uncertainty U_{ij}:

$$\frac{|d_{ij}|}{U_{ij}} < 1. \tag{8}$$

4. Results and discussion

The laser absorption spectroscopy method is applicable at low pressure in most cases since the line broadening increases with pressure and may exceed the laser tuning range. Therefore, the comparison was restricted to low pressure regime. Two nominal reference step pressure Δp of amplitudes 100 kPa and 135 kPa, respectively, were tested. A list of the initial parameters (driven gas pressure, p_1, and driver gas pressure, p_4) and the reflect shock parameters (pressure, p_5, and temperature T_5) at each nominal reference pressure at the two facilities are presented in table 7. The table shows that the driven and the driver gas pressure (p_1 and p_4) employed to achieve the same reference pressure were different at the two facilities. This resulted in a substantial variation in the reflected-shock temperature (T_5) between the two facilities. Hence, the TSs were characterized in a large temperature range (from 500 K to more than 2000 K).

At each facility, the reference step pressure was calculated using the two methods, shock tube model and laser absorption spectroscopy, described in sections 3.1 and 3.2, respectively. A comparison of the values of the reference step pressure calculated by the two methods is depicted in table 8. Thereafter, the dynamic response of the respective TSs in terms of the sensitivity as a function of frequency was calculated according to the procedures described in section 3.3.

In the following, the results for each TS in terms of its sensitivity in the frequency domain at two nominal reference pressure levels of 100 kPa and 135 kPa at each facility will be introduced. Moreover, the degree of equivalence between the results from the two facilities using both the shock tube model and the laser absorption spectroscopy method at each facility will be presented and discussed.

Table 8. A comparison of the values of Δp calculated by using the shock tube model and the laser absorption spectroscopy method at RISE and PTB at two nominal pressure levels of 100 kPa and 135 kPa.

Nominal Δp (kPa)	RISE (ST)	RISE (AS)	PTB (ST)	PTB (AS)
100	102.47 (3.69)	104.05 (4.58)	103.58 (5.87)	103.50 (8.72)
	102.43 (4.10)	103.13 (4.54)	109.49 (6.20)	105.60 (8.90)
	100.37 (4.22)	102.11 (4.50)	107.21 (6.07)	109.69 (9.24)
135	132.87 (3.46)	131.35 (5.78)	139.78 (7.92)	131.51 (11.07)
	133.16 (5.86)	132.83 (5.85)	139.57 (7.90)	144.10 (12.13)
	134.48 (5.65)	133.35 (5.87)	143.57 (8.13)	146.69 (12.35)

The values between parentheses are the expanded uncertainty (k = 2) in the calculated Δp.

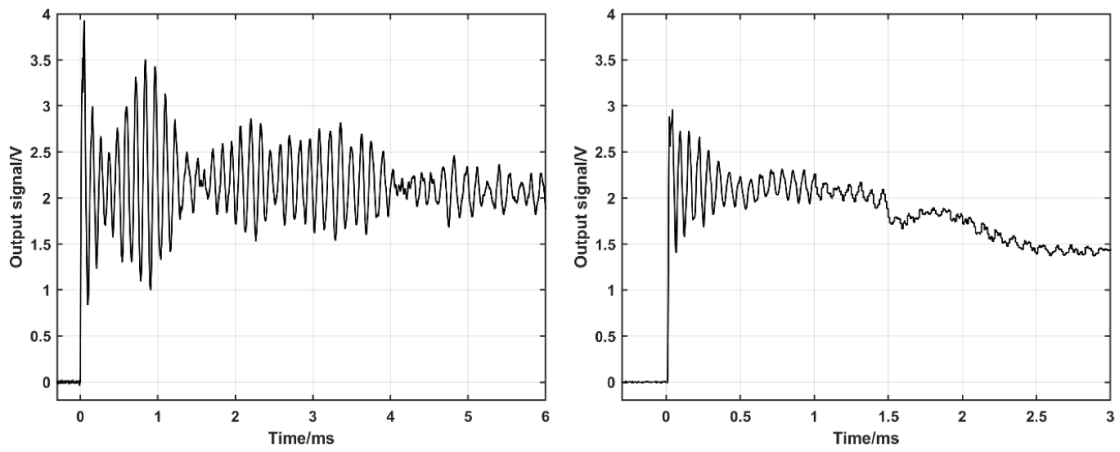

Figure 7. Typical output signals recorded by TS1 at a nominal pressure of 100 kPa at, (a) RISE, (b) PTB.

4.1. TS1

Typical output signals recorded by TS1 (sensor: Kistler 4017 A and signal conditioner: Kistler 4624 A) at a nominal pressure of 100 kPa at RISE and PTB are shown in figures 7(a) and (b), respectively. One can see that the constant-pressure time is about 6 ms at RISE shock tube compared to 1.5 ms at PTB shock tube. This in turn leads to different lower frequency limits that can be generated by the two facilities. Furthermore, oscillations with different characteristic frequencies can be observed in the respective figures. These oscillations originate from the approximately 1.2 cm cavity located in front of the sensor membrane. The cavity behaves as an open–closed acoustic tube, generating a standing wave that limits the dynamic bandwidth of the sensor. The resonance frequency of these oscillations is strongly dependent on the local speed of sound and, consequently, on the temperature of the reflected shock wave. Because the reflected-shock temperature differed between the two facilities at the same nominal reference pressure, see table 7, the resulting oscillation frequencies also differed.

A comparison of the sensitivity of TS1 at nominal reference step pressure of 100 kPa and 135 kPa is shown in Figures 8(a) and 9(a), respectively. While figures 8(b) and 9(b) show zoom in on the corresponding sensitivity up to 3 kHz. A sensitivity close to 21 mV kPa^{-1} can be seen from different methods and facilities. Figure 8(a) shows that there is a peak at 9 kHz and 16 kHz from RISE and PTB measurements, respectively. This peak is due to the standing wave generated in the cavity in front of the membrane of the sensor as described above. The frequency of the standing wave is proportional to the square root of the reflected-shock temperature. Table 7 shows that the temperature of the reflected shock, T_5, at 100 kPa is 2175 K at PTB and 530 K at RISE. The square root of this ratio is about 2, which interprets the discrepancy of the resonance frequency detected by the two facilities. At reference pressure of 135 kHz, the square root of the reflected-shock temperature ratio at the two facilities is 1.4, see table 7. This is in correspondence with the resonance frequency ratio from the results from the two facilities as shown in figure 9(a). The degree of equivalence between the results was estimated using equations (6)–(8) and the results are shown in figures 10 and 11 for the measurements at 100 kPa and 135 kPa, respectively. Figures 10(a) and 11(a) present the degree of equivalence between RISE (shock tube model)

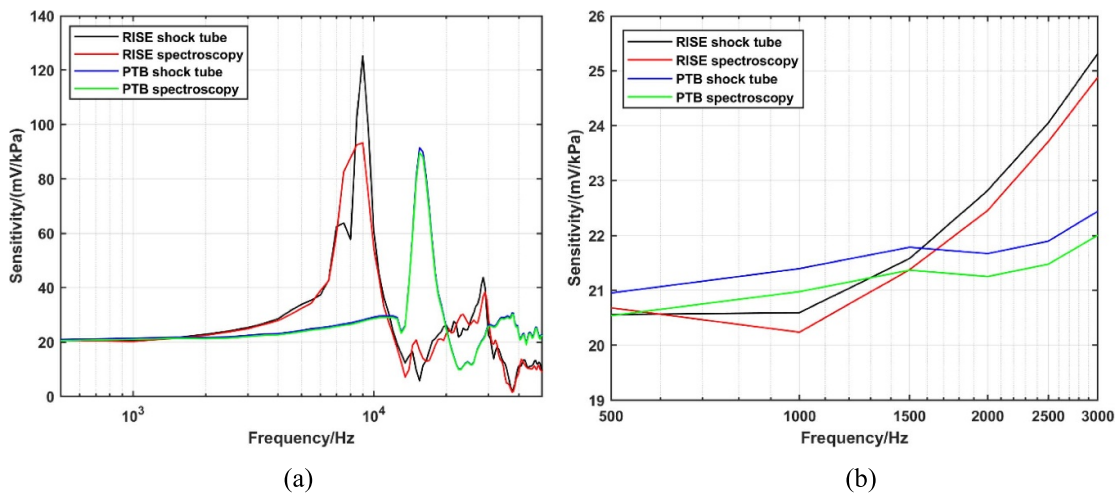

Figure 8. (a) A comparision of the sensitivity as a function of frequency at a nominal pressure of 100 kPa of TS1, (b) Zoom in up to 3 kHz.

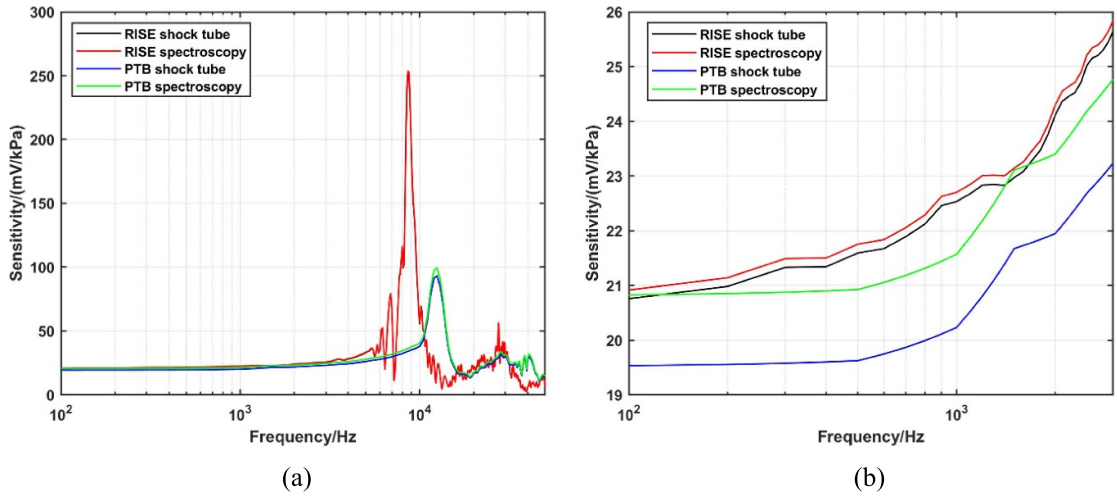

Figure 9. (a) A comparision of the sensitivity as a function of frequency at a nominal pressure of 135 kPa of TS1, (b) Zoom in up to 3 kHz.

and PTB (shock tube model and absorption spectroscopy) at 100 kPa and 135 kPa, respectively. While the degree of equivalence between RISE (absorption spectroscopy) and PTB (shock tube model and absorption spectroscopy) at 100 kPa and 135 kPa are depicted in figures 10(b) and 11(b), respectively. Figures 10(a) and (b) show that there is an equivalence between the results from the two facilities using different methods up to 2 kHz. There is a deviation of the sensitivity calculated using the shock tube model at PTB at 135 kPa, as seen in figure 9(b). This deviation deteriorates the equivalence as can be seen in figures 11(a) and (b). The cause of this deviation has not yet been conclusively identified and is the subject of ongoing investigation. Among the factors currently being examined are the sensor adapter and the mounting conditions at the PTB shock tube for TS1. A summary of the results of TS1, the sensitivity and the degree of equivalence, at a frequency of 0.5 kHz at the two nominal pressure levels is listed in table 9. Furthermore, the sensitivity at a frequency of 0.5 kHz at a nominal pressure of 100 kPa and 135 kPa is depicted in figures 12(a) and (b), respectively.

4.2. TS2

Typical output signals recorded by TS2 (sensor: Kistler 603CAB and charge amplifier: Kistler 5018A1000) at a nominal pressure of 100 kPa at RISE and PTB are shown in figures 13(a) and (b), respectively. From the figures, it can be observed that the constant-pressure duration is approximately 5 ms for RISE shock tube, whereas it is only about 0.5 ms for PTB shock tube. This significant difference in the

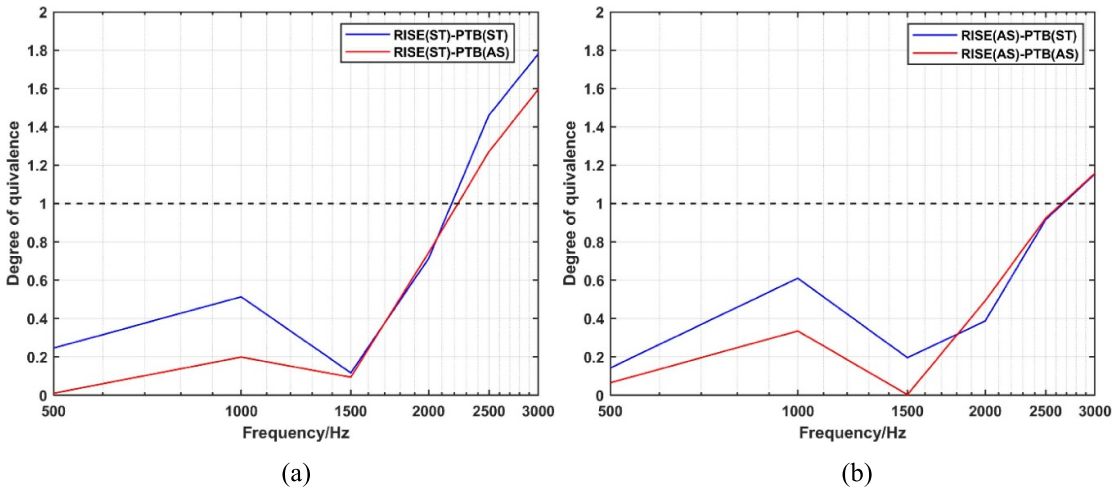

(a) (b)

Figure 10. The degree of equivalence between the measurements at RISE and PTB at a nominal pressure of 100 kPa of TS1, (a) RISE (shock tube model) and PTB (shock tube model and absorption spectroscopy), (b) RISE (absorption spectroscopy) and PTB (shock tube model and absorption spectroscopy).

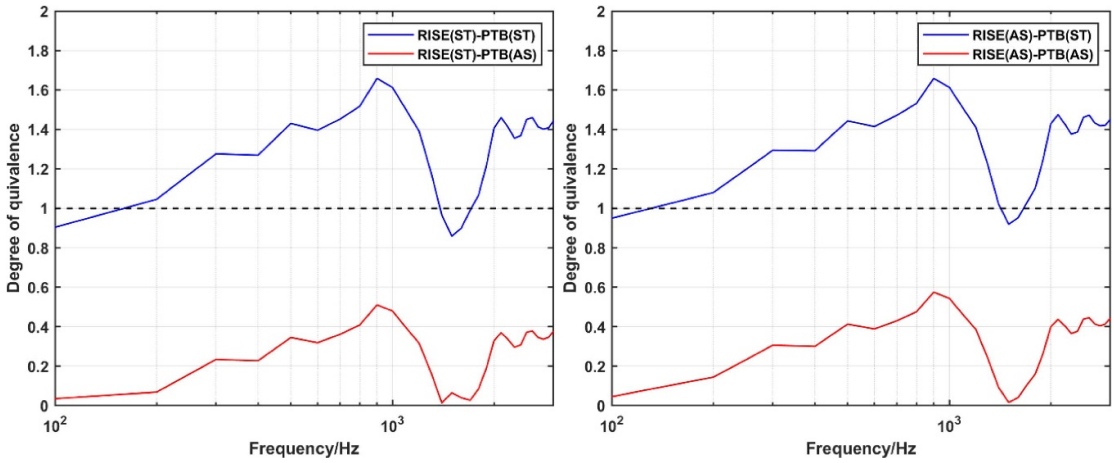

(a) (b)

Figure 11. The degree of equivalence between the measurements at RISE and PTB at a nominal pressure of 135 kPa of TS1, (a) RISE (shock tube model) and PTB (shock tube model and absorption spectroscopy), (b) RISE (absorption spectroscopy) and PTB (shock tube model and absorption spectroscopy).

Table 9. A summary of the results of TS1, the sensitivity and the degree of equivalence, at 0.5 kHz.

Δp (kPa)		100	135
Sensitivity (mV kPa^{-1})	RISE (ST)	20.56 (0.65)	21.59 (0.81)
	RISE (AS)	20.68 (1.23)	21.76 (0.97)
	PTB (ST)	20.95 (1.46)	19.63 (1.11)
	PTB (AS)	20.54 (1.80)	20.93 (1.76)
Equivalence	RISE (ST)—PTB (ST)	0.25	1.43
	RISE (ST)—PTB (AS)	0.01	0.34
	RISE (AS)—PTB (ST)	0.14	1.44
	RISE (AS)—PTB (AS)	0.07	0.41

The values between parentheses are the expanded uncertainty (k = 2) in the calculated sensitivity.

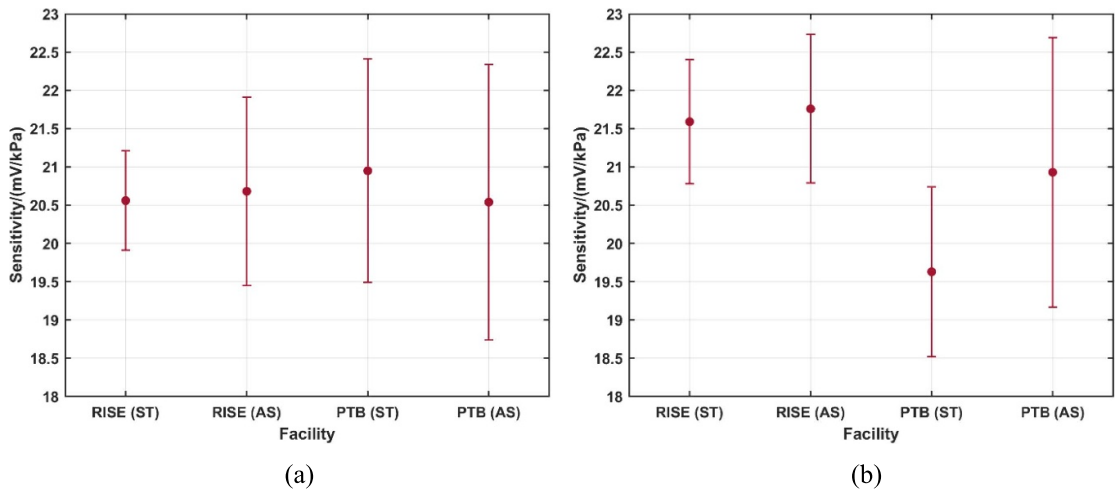

Figure 12. The sensitivity of TS1 at a frequency of 0.5 kHz at nominal pressure of, (a) 100 kPa, (b) 135 kPa.

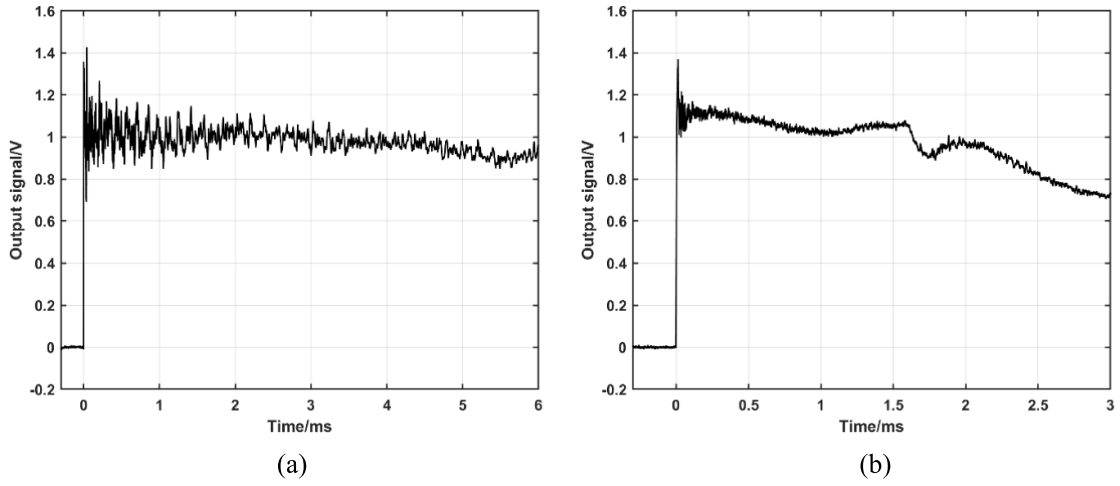

Figure 13. Typical output signals recorded by TS2 at a nominal pressure of 100 kPa at, (a) RISE, (b) PTB.

constant-pressure time has a direct impact on the achievable frequency range of the generated reference pressure at the two facilities. In particular, the much shorter constant-pressure duration at PTB imposes a strong limitation on the generation and reliable characterization of low-frequency components. Consequently, in the determination of the sensitivity of TS2, the results obtained at PTB were extrapolated to extend the analysis into a lower frequency region. This extrapolation was necessary to enable a direct comparison with the sensitivity calculated at RISE, where measurements at low-frequency region were available. Moreover, the figures show that the output signal to noise ratio is lower at RISE compared to PTB.

Following the same procedures as in TS1, the results from TS2 were compared. Figures 14(a) and 15(a) show the sensitivity of TS2 at 100 kPa and 135 kPa, respectively. The corresponding zoom in up to 10 kHz are presented in figures 14(b) and 15(b). From the figures, the sensitivity of the sensor is about 10.5 mV kPa^{-1} and the resonance frequency is >300 kHz. The noise which is pronounced at the frequency region between 10 kHz and 100 kHz at RISE shock tube needs to be investigated. The degree of equivalence between the two facilities are calculated according to equations (6)–(8) and the results are depicted in figures 16 and 17 for results at 100 kPa and 135 kPa, respectively. The figures shows that the results from the two facilities using different methods are equivalent up to 7 kHz. An exception at the frequency region between 0.7 kHz and 2 kHz at 100 kPa when comparing RISE (absorption spectroscopy method) with PTB (shock tube model) can be seen in figure 16(b). A summary of the results of TS2 in terms of the sensitivity and the degree of equivalence at a frequency of 3 kHz is presented in table 10.

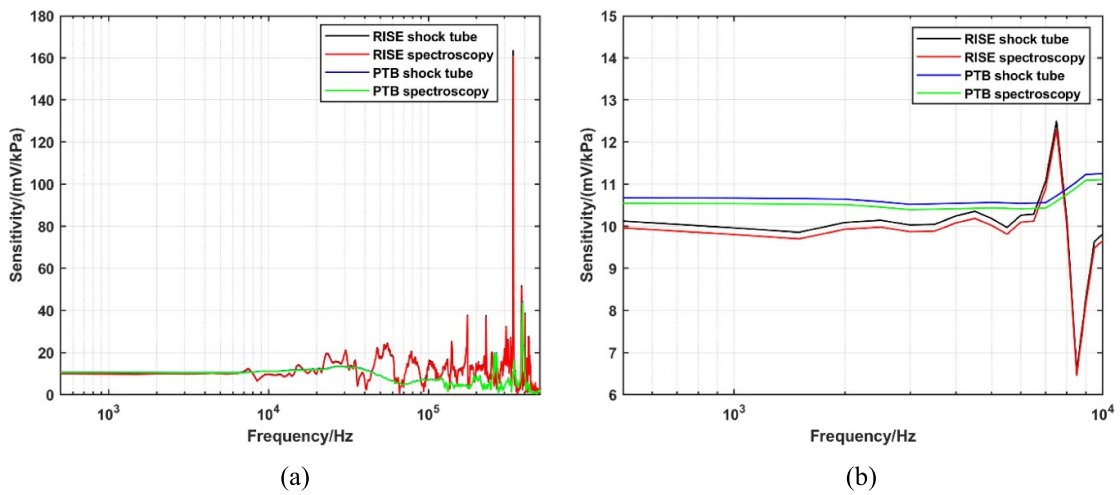

Figure 14. (a) A comparision of the sensitivity as a function of frequency at a nominal pressure of 100 kPa of TS2, (b) Zoom in up to 10 kHz.

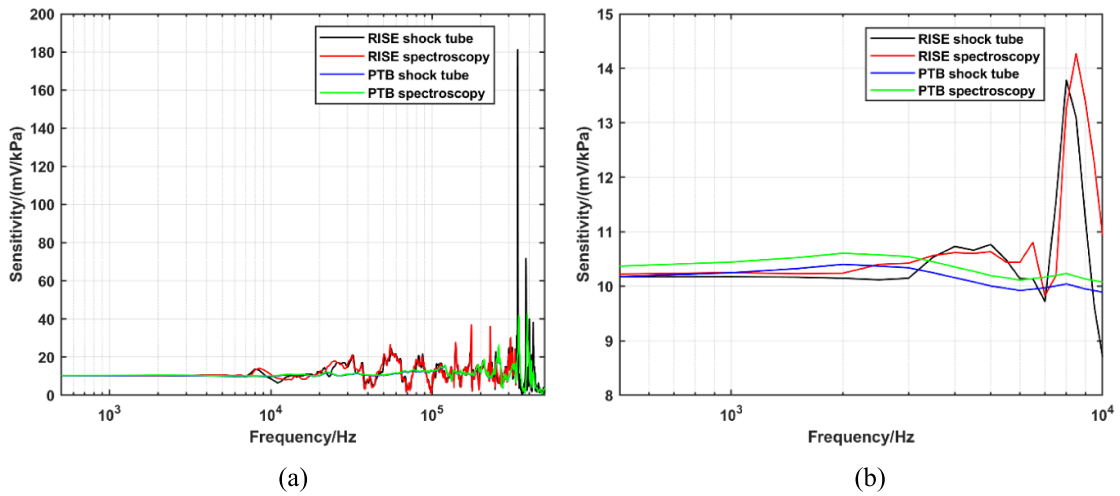

Figure 15. (a) A comparision of the sensitivity as a function of frequency at a nominal pressure of 135 kPa of TS2, (b) Zoom in up to 10 kHz.

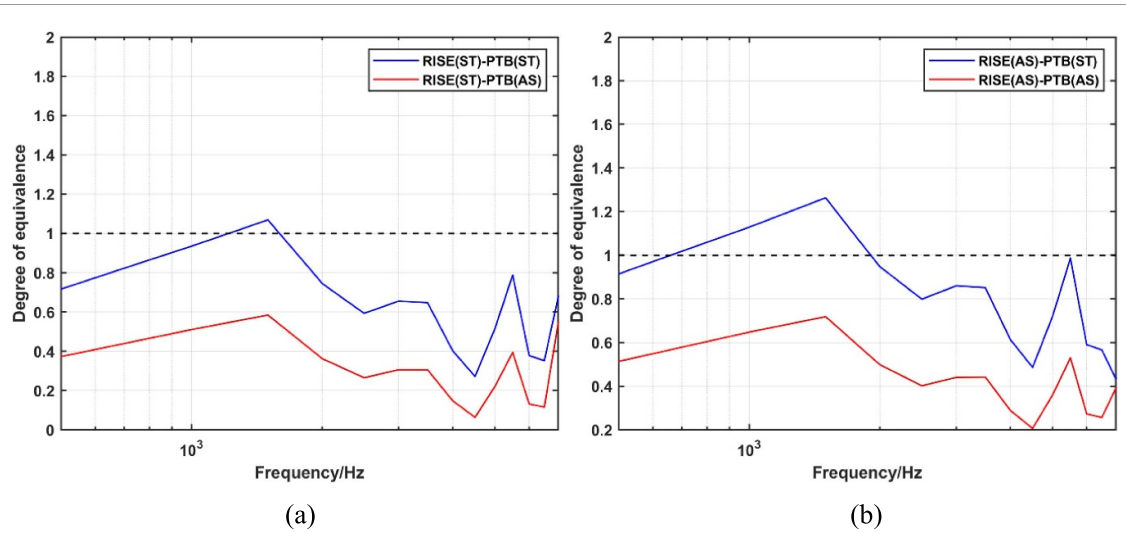

Figure 16. The degree of equivalence between the measurements at RISE and PTB at a nominal pressure of 100 kPa of TS2, (a) RISE (shock tube model) and PTB (shock tube model and absorption spectroscopy), (b) RISE (absorption spectroscopy) and PTB (shock tube model and absorption spectroscopy).

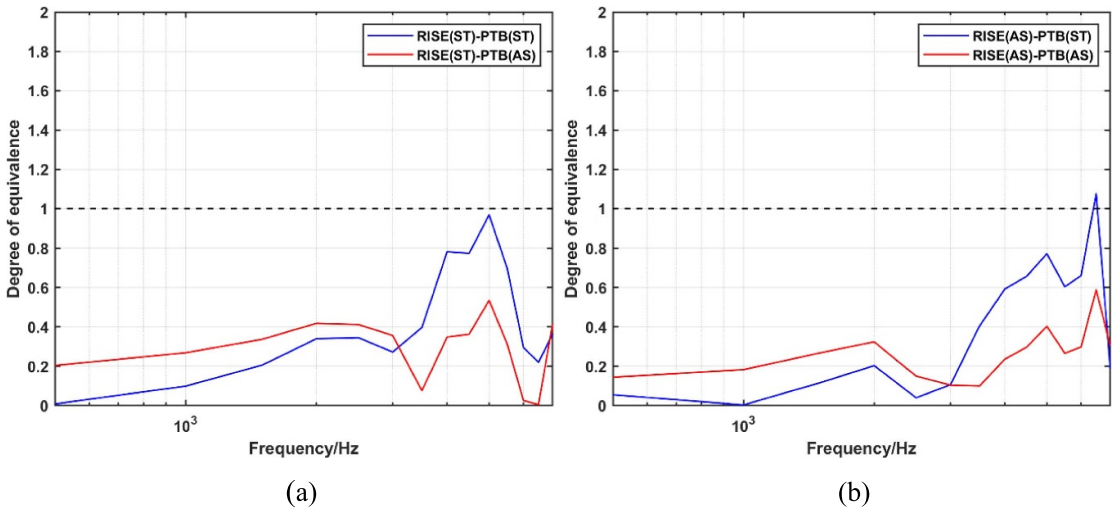

Figure 17. The degree of equivalence between the measurements at RISE and PTB at a nominal pressure of 135 kPa of TS2, (a) RISE (shock tube model) and PTB (shock tube model and absorption spectroscopy), (b) RISE (absorption spectroscopy) and PTB (shock tube model and absorption spectroscopy).

Table 10. A summary of the results of TS2, the sensitivity and the degree of equivalence at a frequency of 3 kHz.

Δp (kPa)		100	135
Sensitivity (mV kPa^{-1})	RISE (ST)	10.03 (0.44)	10.15 (0.39)
	RISE (AS)	9.87 (0.45)	10.42 (0.52)
	PTB (ST)	10.52 (0.61)	10.34 (0.60)
	PTB (AS)	10.40 (1.10)	10.55 (1.05)
Equivalence	RISE (ST)—PTB (ST)	0.66	0.27
	RISE (ST)—PTB (AS)	0.31	0.36
	RISE (AS)—PTB (ST)	0.86	0.10
	RISE (AS)—PTB (AS)	0.44	0.10

The values between parentheses are the expanded uncertainty (k = 2) in the calculated sensitivity.

Moreover, the sensitivity at a frequency of 3 kHz at a nominal pressure of 100 kPa and 135 kPa is shown in figures 18(a) and (b), respectively.

5. Conclusion

In this study, the shock tube facilities at RISE and PTB were validated in the low-pressure regime (up to 200 kPa) and frequency up to 100 kHz through an inter-laboratory comparison employing two TSs (TS1 and TS2). The reference pressure generated at both facilities was determined using two different approaches: the shock tube model and TDLAS. The dynamic responses of the two TSs were calculated at different pressure amplitudes, and the associated uncertainty budgets were evaluated at each facility.

The results demonstrate that TDLAS is a promising technique for achieving traceable dynamic pressure measurements in the low-pressure regime. A good agreement was observed between the reference pressure amplitudes determined using the shock tube model and those obtained from the TDLAS method, with deviations remaining below the combined uncertainty of the respective methods at both RISE and PTB.

Overall, the comparison between the shock tube results obtained at RISE and PTB showed good consistency, despite the presence of some discrepancies. Elevated noise levels were observed in the frequency range between 10 kHz and 100 kHz in the RISE shock tube measurements performed with TS2, indicating that additional investigation is required to identify the origin of these disturbances. Furthermore, the deviation observed in the shock tube model calculations at PTB for TS1 at a pressure level of 135 kPa needs further examination. Additional measurements at this pressure level are therefore necessary to verify the repeatability of the results and to better understand the source of the discrepancy.

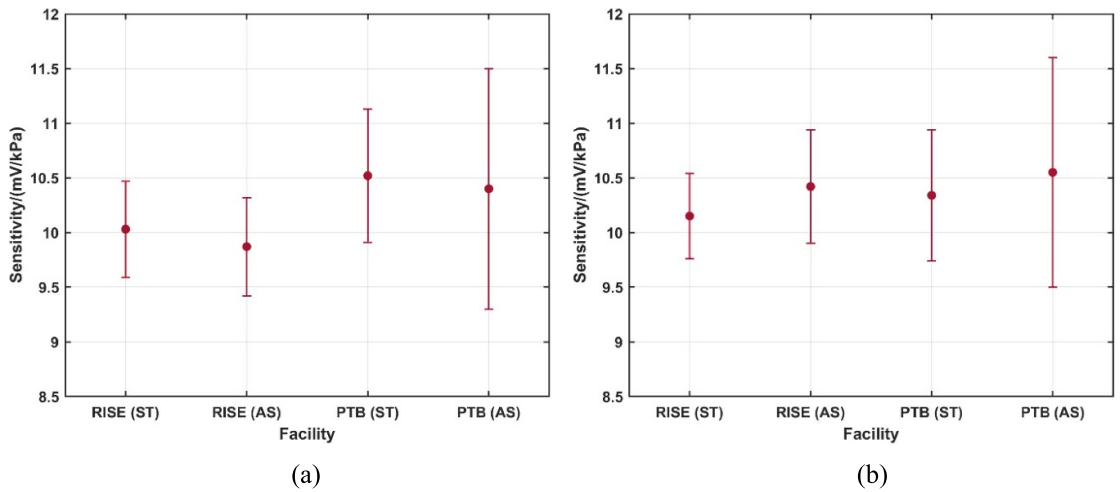

Figure 18. The sensitivity of TS2 at a frequency of 3 kHz at nominal pressure of, (a) 100 kPa, (b) 135 kPa.

Future work will extend the spectroscopic method to higher shock Mach numbers and pressure amplitudes. This extension will require optimization of the selected absorption transition for the expected post-shock pressure and temperature. In particular, line strength, pressure broadening, spectral interference, and laser tuning range must be considered to avoid excessive absorption or saturation while maintaining adequate temporal resolution and signal-to-noise ratio. A key limitation for extending the current method to higher pressures is the availability of a suitable laser source that can scan sufficiently fast while providing a sufficiently broad spectral tuning range to resolve the pressure-broadened absorption feature within the short measurement time. The implementation of wavelength modulation spectroscopy, including normalized $2f/1f$ detection, will also be investigated because of its potential to improve the signal-to-noise ratio. It is therefore a strong candidate for future measurements, especially if weaker transitions must be used at higher pressures to avoid excessive absorption.

Acknowledgment

The financial support by the Swedish Governmental Agency for Innovation Systems, VINNOVA [Grant Numbers 2022-02963] is highly acknowledged.

This research was partially funded by the MaritimeMET (23IND09) project. The project has received funding from the European Partnership on Metrology, co-financed from the European Union's Horizon Europe Research and Innovation Programme and by the Participating States.

The Basic Research Program of Jiangsu under Grant No. BK20251357, and the Start-up Research Fund of Southeast University under Grant RF1028625081 are gratefully acknowledged.

Data availability statement

All data that support the findings of this study are included within the article (and any supplementary files).

Author contributions

Eynas Amer 0000-0003-4853-870X
Conceptualization (equal), Formal analysis (equal), Funding acquisition (equal), Investigation (equal), Software (equal), Writing – original draft (equal), Writing – review & editing (equal)

Denghao Zhu 0000-0002-5055-4496
Conceptualization (equal), Funding acquisition (equal), Investigation (equal), Writing – original draft (equal), Writing – review & editing (equal)

Sumit Agarwal
Investigation (equal), Writing – review & editing (equal)

Fredrik Arrhén
Funding acquisition (equal), Writing – review & editing (equal)

Zhechao Qu 0000-0002-0271-7852
Conceptualization (equal), Funding acquisition (equal), Investigation (equal), Writing – review & editing (equal)

References

[1] Saxholm S *et al* 2018 Development of measurement and calibration techniques for dynamic pressures and temperatures (DynPT): background and objectives of the 17IND07 DynPT project in the European Metrology Programme for Innovation and Research (EMPIR) *J. Phys. Conf. Ser.* **1065** 162015
[2] Amer E, Jönsson G, Penttinen O and Arrhén F 2025 Extending the traceability of dynamic calibration to the high-pressure regime using a shock tube *Sensors* **25** 2453
[3] Amer E, Wozniak M, Jönsson G and Arrhén F 2021 Evaluation of Shock Tube Retrofitted with Fast-Opening Valve for Dynamic Pressure Calibration *Sensors* **21** 4470
[4] Sarraf C and Damion J-P 2018 Dynamic pressure sensitivity determination with Mach number method *Meas. Sci. Technol.* **29** 054006
[5] Salminen J, Högström R, Saxholm S, Lakka A, Riski K and Heinonen M 2018 Development of a primary standard for dynamic pressure based on drop weight method covering a range of 10 MPa–400 MPa *Metrologia* **55** S52
[6] Salminen J, Saxholm S, Hämäläinen J and Högström R 2020 Advances in traceable calibration of cylinder pressure transducers *Metrologia* **57** 045006
[7] Högström R, Lakka A, Hämäläinen J, Salonen L and Brzozowski A 2025 Novel primary standard for dynamic pressure up to 500 MPa *Meas. Sens.* **38** 101686
[8] EMPIR project (available at: www.ptb.de/empir2019/de/quantumpascal/publications/) QuantumPascal
[9] Goldenstein C S, Jeffries J B and Hanson R K 2013 Diode laser measurements of linestrength and temperature-dependent line-shape parameters of H_2O-, CO_2-, and N_2-perturbed H_2O transitions near 2474 and 2482nm *J. Quant. Spectrosc. Radiat. Transf.* **130** 100–11
[10] Goldenstein C S, Spearrin R M, Jeffries J B and Hanson R K 2017 Infrared laser-absorption sensing for combustion gases *Prog. Energy Combust. Sci.* **60** 132–76
[11] Nair A P, Minesi N Q, Kuenning N M, Keller A R and Spearrin R M 2023 Optical pressure sensing at MHz rates via collisional line broadening of carbon monoxide: uncertainty quantification in reacting flows *Appl. Phys. B* **129** 51
[12] Vandervort J A, Schwartz T, Barnes S C, Strand C L and Hanson R K 2024 A laser diagnostic for lineshape-based gas temperature and pressure measurements targeting a single atomic potassium absorption transition *Appl. Phys. B* **130** 117
[13] Gessman I C, Murzyn C M, Swain W E and Daniel K A 2025 Pressure measurements via water vapor absorption spectroscopy for application to post-detonation environments *Appl. Opt.* **64** 5279–85
[14] Douglass K O and Olson D A 2016 Towards a standard for the dynamic measurement of pressure based on laser absorption spectroscopy *Metrologia* **53** S96–S106
[15] HITRAN database 2024 (available at: www.hitran.org/)
[16] Amer E, Jönsson G and Arrhén F 2022 Towards traceable dynamic pressure calibration using a shock tube with an optical probe for accurate phase determination *Metrologia* **59** 035001
[17] Anderson J D 2004 *Modern Compressible Flow* 3rd edn (The Boeing Company)
[18] Zhu D, Seifert L, Agarwal S, Shu B, Ferrnandes R and Qu Z 2025 Measurement of carbon monoxide pressure broadening and temperature dependence coefficients in the $1 \leftarrow 0$ band *Phys. Chem. Chem. Phys.* **27** 7004–15
[19] Farooq A, Jeffries J B and Hanson R K 2008 CO_2 concentration and temperature sensor for combustion gases using diode-laser absorption near 2.7 μm *Appl. Phys. B* **90** 619–28
[20] ISA-37.16.01 2002 *A Guide for Dynamic Calibration of Pressure Transducers 2002* (The Instrumentation, Systems, and Automation Society)
[21] Bipm I, Ifcc I L A C, Iupac I S O and Iupap O I M L 2008 Evaluation of measurement data *Guide to the Expression of Uncertainty in Measurement* vol 100 (Tech rep. JCGM Joint Committee for Guides in Metrology)
[22] Zhu D, Agarwal S, Shu B, Fernandes R and Qu Z 2024 An ultra-rapid optical gas standard for dynamic processes: absolute NH_3 quantification and uncertainty evaluation *Measurement* **230** 114559
[23] Cox M G 2002 The evaluation of key comparison data *Metrologia* **39** 589–95